A bacterial chaperone is required for plastid function in malaria parasites

Anat Florentin[1,2], David W Cobb[1], Jillian D Fishburn[1], Paul S Kim[2], Manuel A Fierro[1], Vasant Muralidharan[1,2*]

[1] Department of Cellular Biology

[2] Center for Tropical and Emerging Global Diseases

University of Georgia, Athens, Georgia, United States of America

* Corresponding author:

E-mail: vasant@uga.edu (VM)

Abstract

Apicomplexan parasites such as *Plasmodium falciparum*, the causative agent of malaria, contain a non-photosynthetic plastid known as the apicoplast that functions to produce essential metabolic compounds. It was previously reported that several members of the Clp family of chaperones and proteases localize to the apicoplast. In bacteria and in chloroplasts these proteins form complexes that degrade proteins in a proteasome-like manner to regulate key cellular processes, but their function in the apicoplast is completely unknown. In this study, we generated a conditional mutant of the *P. falciparum* apicoplast-targeted *pfclpc* gene and found that under normal conditions it localizes to the apicoplast. Knockdown of PfClpC results in growth inhibition and morphological defects, indicating that PfClpC is essential for parasite viability. Upon inhibition, PfClpC loses its apicoplast localization and appears in vesicle-like structures. Other apicoplast-targeted proteins also localize to these structures, suggesting that organelle integrity is compromised. Addition of isopentynyl pyrophosphate completely rescued the growth inhibition, indicating that the only essential function of PfClpC is related to the apicoplast. Moreover, cellular assays suggest that PfClpC inhibition interferes with the ability of the schizont-stage parasites to properly sort functional apicoplast organelles into daughter-merozoites. These data show that PfClpC is an essential gene that functions to maintain apicoplast integrity.

Author Summary

The deadly human malaria parasite, *Plasmodium falciparum*, contains a unique organelle called the apicoplast, a non-photosynthetic plastid that produces vital metabolites. Members of the prokaryotic–derived Clp family were previously reported to localize to the apicoplast. In bacteria and plant chloroplasts, Clp homologs form a proteasome-like complex that degrade proteins but their function in parasite biology is unknown. Here we took a conditional knockdown approach to study an apicoplast localized Clp proteins, PfClpC, which we found to be essential for parasite viability. Inhibition of PfClpC results in a growth arrest phenotype that correlates with a reduced replication rate. We observed that PfClpC localizes to the apicoplast, however upon inhibition it is found dispersed in vesicle-like structures suggesting a complete breakdown of organelle integrity. Our ability to rescue the phenotype by adding an essential apicoplast-derived metabolite proved that the only essential function of PfClpC is linked to apicoplast function. Furthermore, we have found evidence supporting a role for PfClpC in apicoplast sorting into daughter cells. Therefore, we propose PfClpC as a potential drug target due to its essentiality, prokaryotic origin and absence from the human host.

Introduction

Malaria is a devastating human disease caused by obligate intracellular parasites of the genus *Plasmodium*. This disease results in nearly 450,000 deaths each year, which are mostly caused by one species, *Plasmodium falciparum* [1]. The life cycle of the parasite is remarkably complex, moving between different cellular niches in a mosquito vector and in the human host. Upon infection, the parasite initially invades liver cells followed by invasion into red blood cells (RBCs), where the parasite numbers expand exponentially via asexual replication. This part of the cycle initiates with the invasion of a diminutive merozoite into the RBC, developing first into the early ring, then a metabolically active trophozoite, and finally a multinucleated schizont that will give rise to multiple merozoite progeny which egress and reinvade fresh RBCs.

This blood stage form of the parasite is responsible for the entirety of malaria-associated morbidity and mortality. Currently, the parasite has gained resistance to all clinically available antimalarial drugs, generating an urgent need to identify new drugs and potential new drug targets [2,3]. The minute eukaryotic cell of *P. falciparum* is remarkably complex with two organelles that carry their own genetic material, the mitochondrion and a unique algal endosymbiont known as the apicoplast [4]. The apicoplast harbors vital metabolic pathways that are required for parasite growth and survival [5]. Importantly, drugs that target cellular processes in the apicoplast are clinically effective [6-8]. Therefore, understanding the function, structure and biogenesis of the apicoplast are essential areas of research that provide a rich vein of antimalarial drug targets.

The parasite specific and essential nature of the apicoplast makes the development of anti-malarial drugs targeting this organelle extremely attractive. Very little is known about the biogenesis and maintenance of the apicoplast organelle, although factors that are required for or regulate these processes may be an important source of anti-malarial drug targets. One potential class of such targets are the caseinolytic protease (Clp) family of proteins that act as key regulators of the biology of bacterial cells, the evolutionary ancestors of the apicoplast. In bacteria and plant chloroplasts, Clp proteins play vital roles in cell/ organelle division, segregation, protein homeostasis and protein transport [9]. Typically, they form a regulated proteolytic complex in which a Clp protease is paired with a Clp chaperone that has a AAA+ ATPase domain (also known as the Hsp100 family of chaperones) such as ClpC or ClpA [10]. There are several putative *clp* genes encoded in the *P. falciparum* genome and it was recently shown that one of them (PfHSP101) is located at the host-parasite interface and is required to transport parasite virulence factors into the infected host cell [11-13]. Two other Clp proteins have been localized to the mitochondria [14] and six putative Clp's have been localized to the apicoplast [15], yet very little is known about their roles in parasite biology. Although some of their enzymatic activities have been studied *in vitro* [16], their roles *in vivo* remain poorly understood due to the challenging genetics of *P. falciparum* and the difficulty in targeting organelle localized genes for molecular study.

Here we studied the role of the previously uncharacterized PfClpC (PF3D7_1406600), an Hsp100 chaperone with a triple AAA+ ATPase domain.

The *pfclpc* gene is conserved in all *Plasmodium* species, as well as in other apicoplast containing *Apicomplexa*. It encodes a large protein (156 kDa) with a predicted apicoplast transit peptide. Using a conditional knockdown approach, we show that PfClpC activity is essential for parasite survival and growth. Conditional inhibition of PfClpC interferes with apicoplast integrity and the localization of apicoplast proteins. We observe a delayed growth inhibition phenotype, which results from a reduced replication rate that compounds with each subsequent replication cycle. Importantly, we can chemically rescue PfClpC-associated phenotypes using isopentenyl pyrophosphate (IPP) indicating that the only essential role of PfClpC is linked to apicoplast function. Finally, we demonstrate that even after prolonged inhibition and a general apicoplast loss, parasites are able to recover from undetectable levels and grow when PfClpC inhibition is reversed. Overall, we show that PfClpC is a vital apicoplast-targeted protein that is essential for parasite viability through its role in apicoplast function.

Results

Generating conditional mutants of PfClpC

In order to examine the biological role of the putative chaperone PfClpC in apicoplast function and parasite biology, we took a genetic approach based on conditional chaperone auto-inhibition. We inserted a dihydrofolate reductase (DHFR)-based destabilization domain (DDD) into the *pfclpc* genomic locus, a technique that was previously used successfully to conditionally inhibit chaperone function [13,17], as well as to knockdown other *Plasmodium* proteins [18,19] (Fig 1A). In the chaperone-DDD fusion protein, the unfolded DDD binds the chaperone intra-molecularly, thereby excluding client proteins and inhibiting normal chaperone function (Fig 1A). A small molecule ligand, trimethoprim (TMP) is used to stabilize and refold the DDD, releasing the chaperone to resume its normal function (Fig 1A). Using a single crossover homologous recombination strategy, we tagged the C-terminus of the *pfclpc* gene with a triple-hemagglutinin (HA) epitope tag and the DDD (Fig 1B). We isolated two clones from two independent transfections and analyzed the *pfclpc* locus using a southern blot analysis (Fig 1B). Both isolated clones were correctly tagged, and subsequent experiments were done using the two clones, 1G8 and 2E10 (Fig 1B). Henceforth, these parasite lines will also be referred to as PfClpC-DDD.

Using an anti-HA antibody, we confirmed expression of the PfClpC-DDD fusion protein at the expected molecular size in tagged clones but not in the parental line (Fig 1C). The subcellular localization of PfClpC in PfClpC-DDD parasites was observed using immunofluorescence microscopy (Fig 1D). We detected

expression of tagged PfClpC in distinctive structures throughout the asexual blood stages; punctate in early parasites, elongated in mid-stage trophozoites and multiple foci in individual merozoites in the late schizonts stages (Fig 1D).

PfClpC is essential for intraerythrocytic growth of malaria parasites

To test the requirement of PfClpC for parasite growth during the asexual blood stages, we removed the stabilizing ligand (TMP) from culturing media and monitored the growth of unsynchronized PfClpC-DDD parasites. A severe and dramatic growth arrest was seen in parasites after TMP withdrawal (Fig 2A). We found that inhibition of PfClpC relies on TMP in a dose-dependent manner with an EC50 of 80nM (Fig 2B). As expected, based on previously described chaperone-DDD auto-inhibition model, TMP removal did not lead to PfClpC degradation, as protein levels remained constant over time (Fig 2C). Overall, these results demonstrate that PfClpC activity is essential for parasite survival and growth within human RBCs.

PfClpC is required for apicoplast integrity

In order to verify the subcellular localization of PfClpC, we stained cells with anti-HA and anti-acyl carrier protein (ACP), a known apicoplast marker [20], and found that the two co-localize, indicating that under normal conditions PfClpC localizes to the apicoplast (Fig 3A). After TMP removal, we observed that the integrity of the apicoplast was compromised, as observed by staining of PfClpC and ACP (Fig 3B). Inhibition of PfClpC function resulted in loss of the canonical apicoplast

morphology and in the appearance of PfClpC in a punctate, vesicle-like, pattern throughout the cell (Fig 3B). Moreover, this abnormal localization was also observed for ACP, which was detected in similar vesicle-like structures upon PfClpC inhibition, suggesting damage to apicoplast integrity (Fig 3B). Apicoplast targeting of nuclear encoded proteins is mediated through an N-terminal transit peptide that is cleaved in the apicoplast to produce the mature protein [21,22]. In correlation with the mislocalization of PfClpC, a second higher band for PfClpC appeared upon TMP removal, suggesting that the N-terminal transit peptide was not cleaved because it did not reach the apicoplast (S1 Fig).

Intraerythrocytic development requires PfClpC

In agreement with apicoplast dysfunction, PfClpC mutants developed normally during the early stages of rings and trophozoite (S2 Fig), but late schizont stages (≤6 nuclei) developed aberrant morphology, including irregular cellular shape, empty vacuoles and fewer nuclei suggesting that these parasites are nonviable (Fig 4A). These morphologically abnormal parasites appeared on the 3rd replication cycle and their fraction increased over time (Fig 4B). Analysis of the entire population using flow cytometry revealed that instead of a single peak that usually characterizes a synchronized culture, these late-stage parasites had a wider distribution, further suggesting variation in DNA content (Fig 4C). To test the viability and replication efficiency of the mixed parasites population, we used a synchronized culture and monitored the rate of schizonts to ring conversion. In agreement with our previous results showing the presence of morphologically

abnormal schizonts, TMP removal resulted in a significant decrease in the numbers of parasites that were formed in each successive generation (Fig 4D). This reduced replication rate accounts for the observed growth inhibition as well as the increase in the numbers of morphologically abnormal parasites with each generation.

Chemical rescue of PfClpC-DDD parasites using IPP

The only essential function of the apicoplast during the blood stages is the biosynthesis of isopentenyl pyrophosphate (IPP), the precursor for all isoprenoids, through the non-mevalonate pathway [23]. To test the effect of IPP on PfClpC inhibition, we removed TMP and added IPP to the growth media of PfClpC-DDD parasites and observed normal growth as well as typical cellular morphology (Figs 5A and B). Immunofluorescence microscopy revealed that IPP treated PfClpC-DDD parasites survived in the absence of a functional apicoplast and still retained the multiple vesicle-like structures containing PfClpC and ACP (Fig 5C). Moreover, quantitative Real Time PCR (qRT-PCR) analysis supported the visual observation that the apicoplast disappears from these parasites (Fig 5D). Importantly, the mitochondrial genome was not similarly affected by PfClpC inhibition indicating that, in addition to a functional damage to the apicoplast, there was an actual loss of the plastid genome (Fig 5D). Overall, we concluded that the only essential activity of PfClpC is linked to apicoplast function.

The apicoplast is lost from most but not all PfClpC-DDD parasites

In order to link the cellular observation of a morphologically mixed PfClpC-DDD population to the phenotypic evidence of apicoplast dysfunction, we aimed to visualize apicoplast presence or absence in early stage parasites (≤5 hours post invasion). We used Image Stream analysis, which combines flow cytometry with imaging, to analyze these parasites and found that all parasites were positive for PfClpC (S3 Fig and S1 Table). Higher resolution microscopy confirmed that these cells contained PfClpC and that its localization appeared, even in these early stages, in a vesicle-like pattern rather than as a typical discrete apicoplast structure (S4 Fig). This suggests that either newly formed rings inherit these vesicles from their mother cell or that these vesicles represent very early *de novo* synthesis of apicoplast proteins.

Due to the fact that apicoplast proteins are synthesized even in absence of the organelle, they are not indicative of apicoplast loss. Therefore, we employed a functional assay to investigate whether PfClpC inhibition results in a mixed population of parasites with and without an apicoplast. We wanted to know, whether or not a small, yet viable, population of parasites containing an intact and functional apicoplast remained in PfClpC-DDD parasites cultured in the absence of TMP. To test this, we first removed TMP and allowed PfClpC-DDD parasites to grow in the presence or absence of IPP for two weeks (Fig 6A). As expected, PfClpC-DDD parasites grown without TMP and supplemented with IPP grew normally, whereas parasites incubated without TMP and without IPP were unable to grow and were undetectable for several days. On day 14 we removed IPP and relieved PfClpC inhibition by adding back TMP, and monitored the growth of the

parasites (Fig 6B). Upon addition of TMP to the media, parasites grown in the absence of IPP (Fig 6B) recovered and resumed normal growth, indicating that a small fraction of these parasites indeed possessed a functional apicoplast. Conversely, parasites that were grown with IPP started dying 48 hours after removing IPP and adding back TMP (Fig 6B), suggesting that these apicoplast-less parasites through continued growth had outcompeted the few remaining parasites that contained a functional apicoplast. Despite restoration of PfClpC activity, once lost, the parasite is not able to generate, *de novo,* the four-membrane apicoplast. Overall, these data indicate that PfClpC-DDD mutants grown in the absence of TMP lose the apicoplast from most parasite progeny with a small, yet observable population still retaining the plastid.

Discussion

The deadly malaria parasite, *Plasmodium falciparum*, is a eukaryotic pathogen and as such, it shares conserved basic biology with its human host. It is therefore both challenging and essential, in the search for potential drug targets, to identify key components that are absent or significantly different from the human host.

One such potential candidate is the apicoplast-associated prokaryotic Clp family of chaperones and proteases. In the bacterial ancestors, as well as in other organellar descendants such as the mitochondria and chloroplast, these proteins serve a variety of basic molecular functions ranging from protein degradation, transport across membranes, protein folding, cell division, stress response and pathogenicity [24]. These have placed bacterial Clp proteins at the center of several drug discovery programs, and have led to the identification of potent and specific inhibitors [25,26]. Very little is known, however, about the functional roles of the apicoplast-resident Clp proteins in the biology of *Plasmodium falciparum*.

In this study we identified an essential Clp family member, PfClpC, a nuclear encoded gene that is transported to the apicoplast where it is required for the integrity of the organelle. Using a conditional knockdown approach, we demonstrated that PfClpC activity is essential for parasite growth and viability (Figs 1 and 2).

The growth defect of PfClpC-DDD parasites is linked to a failure in apicoplast integrity in several ways. We showed that PfClpC localizes to the apicoplast under normal conditions, but appears, along with other apicoplast proteins, in vesicle like structures upon PfClpC inhibition (Fig 3). Several studies reported the appearance

of such structures when the apicoplast integrity is compromised, for example with the use of certain antibiotics [5,23,27]. This was interpreted as stalled vesicular transport that has left the ER but cannot dock to the apicoplast surface due to loss of the organelle.

Moreover, chemical rescue using IPP restored PfClpC-DDD growth as well as recovered normal cellular morphology (Fig 5). It has been shown that isoprenoid biosynthesis is the only essential metabolic function of the apicoplast, and supplementing IPP can replace a non-functional apicoplast in living parasites [23]. Indeed, the IPP supplemented parasites grew normally but microscopic imaging revealed the presence of punctate structures, which are indicative of apicoplast loss (Fig 5C). This was also supported by qRT-PCR analysis that demonstrated a decrease in the ratio of nuclear to apicoplast genome, highlighting an actual loss of the organelle (Fig 5D). We therefore concluded that the only essential function of PfClpC is linked to apicoplast biology.

Inhibition of essential apicoplast metabolic pathways with drugs like Fosmidomycin, kills parasites immediately and does not lead to the loss of the organelle [28]. Conversely, inhibition of apicoplast translation or replication with drugs like Doxycycline, allows the parasites to complete one asexual cycle, proceed through the second replication cycle, and die only at the schizont stage of the second cycle [7,23]. Similar to the effect of drugs that inhibit apicoplast replication, PfClpC mutants develop normally during the early stages of rings and trophozoite (S2 Fig), but late schizont stages (≤6 nuclei) exhibited aberrant morphology (Figs 4A and C). These non-viable parasites did not manifest

uniformly at the end of the second cycle but appeared on the 3rd replication cycle, and their fraction increased over time (Fig 4B). One possible explanation for the delayed growth arrest, as well as the gradual increase in abnormal parasites, is that PfClpC inhibition interferes with the segregation or division of functional apicoplasts into daughter merozoites. As a consequence, a mixed population of viable and non-viable daughter cells is forming after each cycle, diluting overtime the viable parasites in the total culture. Indeed, we observed a significant decrease in the rate of schizont to ring conversion in each successive generation (Fig 4D), clarifying the delayed growth inhibition, and suggesting a possible defect in apicoplast sorting.

Since most apicoplast resident proteins are encoded by the nucleus [20], they are expressed and sorted into vesicles despite the absence of an apicoplast and therefore could not serve as a proper indicator of apicoplast presence, even in the earliest stages (S3 and S4 Figs and S1 table). We hypothesized that inhibition of PfClpC resulted in an apicoplast segregation or division defect that leads to improper sorting of the organelle into daughter merozoites. Therefore, during every schizogony event only a small fraction of progeny receives an apicoplast from the mother cell. To test the possibility of an apicoplast-related sorting defect, we removed TMP for several replication cycles, inducing persistent growth arrest, and then adding it back and monitoring parasite growth. In the event of a uniform functional damage to all parasites in the culture, PfClpC re-activation would not lead to viable parasites, as *de novo* synthesis of the apicoplast is impossible. Nonetheless, we observed that re-addition of TMP could restore parasites growth,

indicating the presence of a small but undetectable sub-population of parasites that contains a functional apicoplast (Fig 6). This observation further supports a sorting defect rather than a general apicoplast dysfunction in the entire parasite population. Interestingly, TMP addition had the opposite effect on parasites that were rescued with IPP. These parasites started dying 48 hours after removing IPP despite addition of TMP (Fig 6), indicating that re-activation of PfClpC was not enough to sustain viability in a population of parasites that permanently lost the apicoplast. Future work will be needed in order to reveal how exactly PfClpC inhibition affects organelle sorting.

The question remains as to what is the molecular mechanism of PfClpC activity and how does it affect apicoplast function. There are two ClpC homologs in *P. falciparum*, PfClpC that is a nuclear encoded protein targeted to the apicoplast and PfClpM (PFC10_API0060) that is encoded by the apicoplast genome. Our data show that their functions are not redundant and that PfClpC is essential for parasite survival and apicoplast function (Figs 2, 3, 4, and 5). In cyanobacteria and plant chloroplasts, ClpC orthologs, together with a ClpP protease, typically form an ATP-dependent proteolytic complex that degrades proteins to maintain protein homeostasis in the cell/ organelle [10,29]. PfClpC, but not PfClpM, possesses the entire conserved motif that is required to interact with ClpP proteases [30]. The *Plasmodium* ClpP homolog, PfClpP, was shown to have protease activity *in vitro* and localize to the apicoplast *in vivo* [16]. Several other studies provided structural data and binding analysis for two other apicoplast Clp proteins, the inactive protease PfClpR [31] and the adaptor protein PfClpS [32].

As expected, these two proteins have bacterial and chloroplast homologs, which are essential components of the Clp proteolytic complex [31,32]. Interestingly, it was shown that interfering with ClpP activity inhibits cell division in Gram-positive bacteria due to changes in rates of substrate degradation [33]. Further studies are required in order to understand whether a similar complex is indeed formed in the apicoplast of *P. falciparum*, and whether it plays an essential role in maintaining a functional apicoplast. Such investigation may reveal the link between the apicoplast sorting defect and the proteolytic ClpP/C complex in the form of unknown substrate/s that need to be degraded in order to facilitate proper organelle division and segregation.

Fig 1: Generating PfClpC-DDD Conditional Mutants.

A. Mechanism of PfClpC conditional inhibition. The *pfclpc* locus was modified to contain a triple hemagglutinin (HA) tag and a DHFR-based destabilization domain (DDD). In the presence of trimethoprim (TMP) the DDD is stable and the chaperone is active. Upon TMP removal the chaperone binds the DDD intra-molecularly and cannot interact with client proteins, inhibiting normal activity.

B. Single crossover homologous recombination enables the integration of the plasmid into the 3' end of the *pfclpc* gene (upper panel). Southern blot analysis of genomic DNA (bottom panel) isolated from parasite lines indicated above the lanes. The genomic DNA was digested with NcoI and XmnI. Bands expected from integration of the plasmid into the 3' end of the *pfclpc* gene were observed in two clones (1G8 and 2E10), isolated from two independent transfections (Red). A plasmid band was observed in the clones (blue), suggesting that a plasmid concatamer integrated into the gene. A single band indicative of the parental allele was observed for the parental strain (black) and it was absent in the integrant clones.

C. Western blot of parasite lysates from parental line and two independent clones (1G8 and 2E10) probed with antibodies against HA (green) and EF1α (loading control, red). The protein marker sizes that co-migrated with the probed protein are shown on the left.

D. Immunofluorescence imaging of fixed unsynchronized PfClpC-DDD parasites stained with antibodies against HA (green) and DAPI (blue). Z-stack images were

deconvolved and projected as a combined single image. Scale bar, 5μ□. One representative experiment out of four (two for each clone) is shown.

Fig 2: PfClpC Activity is Essential for Parasite Growth.

A. Asynchronous PfClpC-DDD clones, 1G8 and 2E10, were grown with or without 10μM TMP and parasitemia was monitored every 24 hours over 12 days via flow cytometry. During the course of the experiment cultures were cut back and data were calculated using the actual parasitemia multiplied by the dilution factors of each individual culture. 100% of relative parasitemia represents the highest value of calculated parasitemia. Growth inhibition is observed after 7-8 days post TMP removal, corresponding to roughly 3-4 asexual cycles. Data are fit to an exponential growth equation and are represented as mean ± S.E.M. (n=3). One representative experiment out of three is shown.

B. Asynchronous PfClpC-DDD parasites were incubated for 11 days without TMP, and on day 12 were seeded in a 96 well plate with varying concentrations of TMP. Parasitemia was measured after 5 days using flow cytometry showing an EC50 of 80nM. Data are fit to a dose-response equation and are represented as mean ± S.E.M. (n=3). One representative experiment out of four is shown.

C. TMP was removed from PfClpC-DDD parasites and parasite lysates were isolated every 24 or 48 hours over 11 days. PfClpC and EF1α were visualized on Western blots using antibodies against HA (PfClpC-DDD, green) and EF1α (loading control, red). The protein marker sizes that co-migrated with the probed

protein are shown on the left. One representative experiment out of four is shown (two for each clone).

Fig 3: PfClpC Inhibition Disrupts the Localization of Apicoplast Proteins

A. PfClpC-DDD parasites were fixed and stained with antibodies against HA (red) and ACP (green). Both clones of PfClpC-DDD parasites are shown, indicated next to the images. Images from left to right are anti-HA, anti-ACP, DAPI, fluorescence merge and phase. Z-stack images were deconvolved and projected as a combined single image. Scale bar, 5µM.

B. PfClpC-DDD parasites were incubated for 10 days without TMP and then fixed and stained with antibodies against HA (red), ACP (green) and DAPI (blue). Both clones of PfClpC-DDD parasites are shown, indicated next to the images. Images from left to right are anti-HA, anti-ACP, DAPI, fluorescence merge and phase. Z-stack images were deconvolved and projected as a combined single image. Scale bar, 5µM.

C.

Fig 4: PfClpC Inhibition is Associated with Reduced Replication Efficiency

A. Hema 3 stained thin blood smears of PfClpC-DDD parasites that were grown for 10 days without TMP. Both clones of PfClpC-DDD parasites are shown, as indicated above the images.

B. TMP was removed from synchronized PfClpC-DDD parasites and thin blood smears of late stage schizonts were stained and analyzed using light microscopy. Parasites were counted, and the fraction of defective cells (as seen

in 4A) was calculated out of the total late-stage population (≤6 nuclei). Data are shown from one representative experiment with clone 2E10. Two experiments (with technical triplicates) were performed with each clone.

C. TMP was removed from synchronized PfClpC-DDD parasites and the DNA of the parasites was stained using Acridine Orange and was analyzed by flow cytometry during the 6th replication cycle. One representative image is shown (out of four experiments, two with each clone).

D. TMP was removed from synchronized PfClpC-DDD parasites and the numbers of rings and late schizont stages was determined by flow cytometry. The ratio of rings to schizonts was calculated using the number of rings arising from schizonts in the previous generation. Cultures were re-synchronized at the beginning of each replication cycle using sorbitol. Data were normalized to the ring: schizont ratio in the presence of TMP. Data are shown for 1G8 clone. The experiment was performed twice for each clone (with technical triplicates in each experiment).

Fig 5: IPP Rescues PfClpC Auto-inhibition

A. PfClpC-DDD parasites were grown for 10 days without TMP and supplemented with isopentenyl pyrophosphate (IPP). Parasitemia was measured using flow cytometry. During the course of the experiment cultures were subcultured and data were calculated using the actual parasitemia multiplied by the dilution factors of each individual culture. 100% of relative parasitemia represents the highest value of calculated parasitemia at the end of the experiment. Data are fit

to an exponential growth equation and are represented as mean ± S.E.M. (n=3). One of two (one for each clone) representative experiments is shown. Graph denotes data collected for 1G8 clone.

B. Hema 3 stained thin blood smears of PfClpC-DDD parasites (1G8 clone) grown for 10 days with TMP (upper), without TMP (middle) or without TMP and supplemented with IPP (bottom). Two representative images for each condition are shown.

C. PfClpC-DDD parasites (1G8 clone) grown for 10 days without TMP and supplemented with IPP. These PfClpC-DDD parasites were fixed and stained with antibodies against HA (red) and ACP (green). Images from left to right are anti-HA, anti-ACP, DAPI, fluorescence merge and phase. Z-stack images were deconvolved and projected as a combined single image. Scale bar, 5µM.

D. Synchronized PfClpC-DDD parasites were grown in the absence of TMP and presence of IPP and DNA samples were taken at the beginning of each replication cycle for quantitative Real Time PCR analysis. Apicoplast: nuclear genome ratio was calculated for each replication cycle. Mitochondria: nuclear genome ratio served as a control. Genome ratios were normalized to parasites grown in the presence of TMP. Data are represented as mean ± S.E.M (n=3) from one representative experiment (out of four, two for each clone).

E.

Fig 6: PfClpC Inhibition is Reversible

A. PfClpC tagged parasites were grown for 14 days without TMP (red line), or without TMP and supplemented with IPP (green line). During the course of the

experiment cultures were subcultured and data were calculated using the actual parasitemia multiplied by the dilution factors of each individual culture. 100% of relative parasitemia represents the highest value of calculated parasitemia at the end of the experiment. Data are fit to an exponential growth equation and are represented as mean ± S.E.M. (n=3). One representative experiment out of two for each clone is shown.

B. On day 14 IPP was removed from the media and TMP was added back to all parasite cultures and parasitemia was measured using flow cytometry. 100% of relative parasitemia represents the highest parasitemia value at the beginning of the experiment. Data are represented as mean ± S.E.M. (n=3). One representative experiment out of two for each clone is shown.

S1 Fig: PfClpC Auto-inhibition Interferes with Transit Peptide Processing

TMP was removed from PfClpC-DDD parasites and parasite lysates were isolated every 24 to 48 hours over 13 days. PfClpC and Plasmepsin V (PMV) were visualized on Western blots using antibodies against HA (PfClpC-DDD) and PMV (loading control).

S2 Fig: PfClpC inhibition does not affect early stage development

Hema 3 stained thin blood smears of early stage PfClpC-DDD parasites that were grown for 10 days without TMP. Both clones of PfClpC-DDD parasites are shown, indicated above the images.

S3 Fig: Early Stage PfClpC-DDD parasites are positive for HA

Synchronized PfClpC-DDD parasites incubated for 10 days without TMP. Schizont stage parasites were isolated on a percoll gradient following by a sorbitol treatment 5 hours later to obtain early rings (0-5 hours post invasion). Parasites were fixed and stained with DAPI to visualize DNA and antibodies against HA to observe PfClpC-DDD. Parasites were detected using Imaging flow cytometry (ImageStream). Images from left to right are anti-HA, DAPI, fluorescence merge and phase. Representative images of fixed parasitized RBCs as observes via the imaging flow cytometry.

Clone/ condition	Infected cells positive for HA (%)
1G8+TMP	99.76
1G8-TMP	96.93
2E10+TMP	99.62
2E10-TMP	98.96

S1 Table: Early Stage PfClpC-DDD Parasites are Positive for HA

Synchronized PfClpC-DDD parasites incubated for 10 days without TMP. Schizont stage PfClpC-DDD parasites were isolated on a percoll gradient following by a sorbitol treatment 5 hours later to obtain early rings (0-5 hours post invasion). Parasites were fixed and stained with DAPI to visualize DNA and antibodies against HA to observe PfClpC-DDD. Parasites were detected using Imaging flow cytometry (ImageStream). The able shows a summary of the results as percentage of parasitized RBCs positive for HA staining.

S4 Fig: Vesicle-like Structures are Present in Early Stage PfClpC-DDD Parasites

Synchronized PfClpC-DDD parasites incubated for 10 days without TMP. Schizont stage parasites were isolated on a percoll gradient following by a sorbitol treatment 5 hours later to obtain early rings (0-5 hours post invasion). Parasites were fixed and stained with DAPI to visualize DNA and antibodies against HA to observe PfClpC-DDD. Images from left to right are phase, anti-HA, anti-ACP, DAPI, and fluorescence merge. Z-stack images were deconvolved and projected as a combined single image. Scale bar, 5μM.

Materials and Methods

Plasmid construction

Genomic DNAs were isolated from *P. falciparum* using the QIAamp DNA blood kit (QIAGEN). Constructs utilized in this study were confirmed by sequencing. PCR products were inserted into the respective plasmids using the In-Fusion cloning system (Clonetech). For generation of PfClpC-DDD a 1-kb homologous sequence from the 3'-end of the *pfclpc* gene (not including the stop codon) was amplified by PCR using primers 5'-cactatagaactcgagCCAAATAAACCTATTGGTACTCTTCTATTATGTGGTTCATCAGG-3' and 5'-cgtatgggtacctaggAGATGAAAATTGTTGAACTGGTGCTTTTATTAATTGTACTTTAA-3' and was inserted into pHADB [13] using restriction sites XhoI and AvrII (New England Biolabs).

Parasite culture and transfections

Commercially purchased de-identified and anonymized units of human blood were utilized for growing *P. falciparum* (Interstate Blood Bank, Memphis, TN). Parasites were grown in human red blood cells at 2% hematocrit in RPMI medium supplemented with Albumax I (Gibco) and transfected as described earlier [34,35]. pPfClpC-HADB was transfected in duplicates into 3D7-derived parental strain PM1KO which contains a hDHFR expression cassette conferring resistance to TMP [36]. Selection, drug cycling and cloning were performed as described [17] in the presence of 10 μM of TMP (Sigma). Integration was detected after one round of drug cycling with blasticidin (Sigma). Two clones

from 2 independent transfections, 1G8 and 2E10, were isolated via limiting dilutions and used for subsequent experiments.

For IPP rescue, media was supplemented with 200 μM of IPP (Isoprenoids LC) in PBS.

Growth assays

For asynchronous growth assays parasites were washed twice and incubated in the required medium. Throughout the course of the experiment parasites were sub-cultured to avoid high parasite density and parasitemia was monitored every 24 hours via flow cytometry. Relative parasitemia at each time point was back calculated based on actual parasitemia multiplied by the relevant dilution factors. Parasitemia in the presence of TMP at the end of each experiment was set as the highest relative parasitemia and was used to normalize parasites growth. Data were fit to exponential growth equations using Prism (GraphPad Software, Inc.)

To generate an EC50 curve for TMP, asynchronous PfClpC-DDD parasites were incubated for 11 days without TMP, and on day 12 were seeded in a 96 well plate with varying concentrations of TMP. Parasitemia was measured after 5 days using flow cytometry. Data were fit to a dose-response equation using Prism (GraphPad Software, Inc.).

To determine replication rate (rings: schizonts ratio), TMP was removed from percoll-isolated schizonts-stage parasites and parasites were allowed to egress and reinvade fresh RBCs. Parasitemia was monitored by flow cytometry and microscopy. The ratio of rings to schizonts was calculated using number of rings

arising from schizonts in the previous generation. At the beginning of each replication cycle parasites were re-synchronized using Sorbitol, and sub-cultured when required. For each replication cycle data were normalized to rings: schizonts ratio in the presence of TMP.

To determine the fraction of morphologically aberrant schizonts thin blood smears of synchronized PfClpC-DDD parasites were performed at the final stages of each replication cycle and the fraction of defective cells was calculated based on the total late schizont stage parasite counts.

Southern blot

Southern blots were performed with genomic DNA isolated using the Qiagen Blood and Cell Culture kit. 10 μg of DNA was digested overnight with NcoI and XmnI (New England Biolabs) and integrants were screened using biotin-labeled probes against the 3'-end of the *pfclpc* ORF. Southern blot was performed as described earlier [37]. The probe was labeled using biotinylated Biotin-16-dUTP (Sigma). The biotinylated probe was detected on blots using IRDye 800CW Streptavidin conjugated dye (LICOR Biosciences) and was imaged, processed and analyzed using the Odyssey infrared imaging system software (LICOR Biosciences).

Western blot

Western blots were performed as described previously [18]. Briefly, parasites were collected and host red blood cells were permeabilized selectively by treatment with ice-cold 0.04% saponin in PBS for 10 min, followed by a wash in ice-cold PBS. Cells were lysed using RIPA buffer, sonicated, and cleared by

centrifugation at 4°C. The antibodies used in this study were rat monoclonal anti-HA, 3F10 (1:3000) (Roche), mouse monoclonal anti-PMV (from D. Goldberg, 1: 400) and rabbit polyclonal anti-EF1α (from D. Goldberg, 1: 2000). The secondary antibodies that were used are IRDye 680CW goat anti-rabbit IgG and IRDye 800CW goat anti-mouse IgG (LICOR Biosciences, 1:20,000). The Western blot images were processed and analyzed using the Odyssey infrared imaging system software (LICOR Biosciences).

Microscopy and image processing

For IFA cells were fixed using a mix of 4% Paraformaldehyde and 0.015% glutaraldehyde and permeabilized using 0.1% Triton-X100. Primary antibodies used are rat anti-HA clone 3F10 (Roche, 1:100) and rabbit anti-ACP (from G. Mcfadden, 1:10,000). Secondary antibodies used are Alexa Fluor 488 and Alexa Fluor 546 (Life Technologies, 1:100). Cells were mounted on ProLong Diamond with DAPI (Invitrogen) and were imaged using DeltaVision II microscope system with an Olympus IX-71 inverted microscope using a 100X objective. All images were collected as Z-stack, were deconvolved using the DVII acquisition software SoftWorx and displayed as maximum intensity projection. Image processing, analysis and display were preformed using SoftWorx and Adobe Photoshop. Adjustments to brightness and contrast were made for display purposes. Thin blood smears were stained using Hema 3 stain set (PRTOCOL/ Fisher Diagnostics) and were imaged on a Nikon Eclipse E400 microscope.

Flow cytometry

Aliquots of parasite cultures (5 μl) were stained with 1.5 mg/ml Acridine Orange (Molecular Probes) in PBS. The fluorescence profiles of infected erythrocytes were measured by flow cytometry on a CyAn ADP (Beckman Coulter, Hialeah, Florida) and analyzed by FlowJo software (Treestar, Inc., Ashland, Oregon). The parasitemia data were fit to standard growth curve or dose–response using Prism (GraphPad Software, Inc.).

Quantitative Real Time PCR

Synchronized ring stage parasites samples were collected at the beginning of each replication cycle and genomic DNA was isolated by saponin lysis to remove extracellular DNA. Genomic DNA was purified using QIAamp blood kits (Qiagen). Primers that amplify segments from genes encoded by nuclear or organelles genomes were designed using RealTime qPCR Assay Entry (IDT). *cht1* (nuclear): 5'-TCCATTGGTGATTTTGTAAAGACTG-3' and 5'-CTAATTGTTCATTATGTGCAGCATTATC-3'. *tufA* (apicoplast): 5'-AATTAACACAAGCACAATCCGG-3' and 5'- GGTTTATGACGACCACCTTCT-3'. *cytb3* (mitochondria): 5'- CTGCTTTCGTTGGTTATGTCTTAC-3' and 5'-CTCACAGTATATCCTCCACATATCC-3'. Reactions contained template DNA, 0.5 μM of gene specific primers, and IQ™ SYBR Green Supermix (BIORAD). Quantitative real-time PCR was carried out in triplicates and was performed at a 2-step reaction with 95°C denaturation and 56°C annealing and extension for 35 cycles on a CFX96 Real-Time System (BIORAD). Relative quantification of target genes was determined using Bio-Rad CFX manager 3.1 software. Standard curves for each primers set were obtained by using different dilutions of control

gDNA isolated from parasites grown in the presence of TMP (20 to 0.2 ng) as template, and these standard curves were used to determine primers efficiency. For each replication cycle number, the organelle: nuclear genome ratio of the –TMP+IPP treated parasites was calculated relative to that of the +TMP control.

Imaging flow cytometry

Synchronized PfClpC-DDD parasites incubated for 10 days without TMP and then were isolated on a percoll gradient following by a sorbitol treatment 5 hours later to obtain early rings (0-5 hours post invasion). Cells were fixed and stained with anti HA antibody as described above and nuclei were stained using DAPI from Amnis Intracellular staining kit (EMD MILIPORE). Data were collected on ImageStream X Mark II (EMD MILIPORE) and an automated collection of a statistically large number of cells (10,000) was performed. Data were analyzed using IDEAS software version 6.2.

Acknowledgements

We thank Geoffrey McFadden for anti-ACP antibody and Dan Goldberg for anti-PMV and anti EF1α antibodies; Drew Etheridge for comments on the manuscript; Julie Nelson at the CTEGD Cytometry Shared Resource Laboratory for help with flow cytometry and analysis; and Muthugapatti Kandasamy at the Biomedical Microscopy Core at the University of Georgia for help with microscopy. We acknowledge the assistance of the Children's Healthcare of Atlanta and Emory University Pediatric Flow Cytometry Core for imaging flow cytometry.

References

1. World Health Organization. World Malaria Report 2015. WHO, Geneva. 2015.

2. Hovlid ML, Winzeler EA. Phenotypic Screens in Antimalarial Drug Discovery. Trends Parasitol. 2016;32: 697–707.

3. Wells TNC, van Huijsduijnen RH, Van Voorhis WC. Malaria medicines: a glass half full? Nat Rev Drug Discov. 2015;14: 424–442.

4. McFadden GI. Plastid in human parasites. Nature. 1996;381: 482–482.

5. van Dooren GG, Striepen B. The algal past and parasite present of the apicoplast. Annu Rev Microbiol. 2013;67: 271–289.

6. Goodman CD, Su V, McFadden GI. The effects of anti-bacterials on the malaria parasite Plasmodium falciparum. Mol Biochem Parasitol. 2007;152: 181–191.

7. Fichera ME, Roos DS. A plastid organelle as a drug target in apicomplexan parasites. Nature. 1997;390: 407–409.

8. Dahl EL, Rosenthal PJ. Multiple Antibiotics Exert Delayed Effects against the Plasmodium falciparum Apicoplast. Antimicrob Agents Chemother. 2007;51: 3485–3490.

9. Trösch R, Mühlhaus T, Schroda M, Willmund F. ATP-dependent molecular chaperones in plastids — More complex than expected. Biochim Biophys Acta. 2015;1847: 872–888.

10. Nishimura K, van Wijk KJ. Organization, function and substrates of the essential Clp protease system in plastids. Biochim Biophys Acta. 2015;1847: 915–930.

11. Elsworth B, Matthews K, Nie CQ, Kalanon M, Charnaud SC, Sanders PR, et al. PTEX is an essential nexus for protein export in malaria parasites. Nature. 2014;511: 587–591.

12. de Koning-Ward TF, Gilson PR, Boddey JA, Rug M, Smith BJ, Papenfuss AT, et al. A newly discovered protein export machine in malaria parasites. Nature. 2009;459: 945–949.

13. Beck JR, Muralidharan V, Oksman A, Goldberg DE. PTEX component HSP101 mediates export of diverse malaria effectors into host erythrocytes. Nature. 2014;511: 592–595.

14. Jain S, Rathore S, Asad M, Hossain ME, Sinha D, Datta G, et al. The

prokaryotic ClpQ protease plays a key role in growth and development of mitochondria in Plasmodium falciparum. Cell Microbiol. 2013;15: 1660-73

15. Bakkouri El M, Pow A, Mulichak A, Cheung KLY, Artz JD, Amani M, et al. The Clp chaperones and proteases of the human malaria parasite Plasmodium falciparum. J Mol Biol. 2010;404: 456–477.

16. Rathore S, Sinha D, Asad M, Böttcher T, Afrin F, Chauhan VS, et al. A cyanobacterial serine protease of Plasmodium falciparum is targeted to the apicoplast and plays an important role in its growth and development. Mol Microbiol. 2010;77: 873–890.

17. Muralidharan V, Oksman A, Pal P, Lindquist S, Goldberg DE. Plasmodium falciparum heat shock protein 110 stabilizes the asparagine repeat-rich parasite proteome during malarial fevers. Nat Commun. 2012;3: 1310.

18. Muralidharan V, Oksman A, Iwamoto M, Wandless TJ, Goldberg DE. Asparagine repeat function in a Plasmodium falciparum protein assessed via a regulatable fluorescent affinity tag. Proc Natl Acad Sci. 2011;108: 4411–4416.

19. Nacer A, Claes A, Roberts A, Scheidig Benatar C, Sakamoto H, Ghorbal M, et al. Discovery of a novel and conserved Plasmodium falciparum exported protein that is important for adhesion of PfEMP1 at the surface of infected erythrocytes. Cell Microbiol. 2015;17: 1205–1216.

20. Waller RF, Keeling PJ, Donald RG, Striepen B, Handman E, Lang-Unnasch N, et al. Nuclear-encoded proteins target to the plastid in Toxoplasma gondii and Plasmodium falciparum. Proc Natl Acad Sci. 1998;95: 12352–12357.

21. Foth BJ, Ralph SA, Tonkin CJ, Struck NS, Fraunholz M, Roos DS, et al. Dissecting Apicoplast Targeting in the Malaria Parasite Plasmodium falciparum. Science. 2003;299: 705–708.

22. Waller RF, Reed MB, Cowman AF, Mcfadden GI. Protein trafficking to the plastid of Plasmodium falciparum is via the secretory pathway. EMBO J. 2000;19: 1794–1802.

23. Yeh E, DeRisi JL. Chemical rescue of malaria parasites lacking an apicoplast defines organelle function in blood-stage Plasmodium falciparum. PLoS Biol. 2011;9: e1001138.

24. Frees D, Gerth U, Ingmer H. Clp chaperones and proteases are central in stress survival, virulence and antibiotic resistance of Staphylococcus aureus. Int J Med Microbiol. 2014;304: 142–149.

25. Böttcher T, Sieber SA. β-Lactones as Specific Inhibitors of ClpP Attenuate

the Production of Extracellular Virulence Factors of Staphylococcus aureus. J Am Chem Soc. 2008;130: 14400–14401.

26. Brötz-Oesterhelt H, Sass P. Bacterial caseinolytic proteases as novel targets for antibacterial treatment. Int J Med Microbiol. 2014;304: 23–30.

27. Gisselberg JE, Dellibovi-Ragheb TA, Matthews KA, Bosch G, Prigge ST. The suf iron-sulfur cluster synthesis pathway is required for apicoplast maintenance in malaria parasites. PLoS Pathogens. 2013;9: e1003655.

28. Bowman JD, Merino EF, Brooks CF, Striepen B, Carlier PR, Cassera MB. Antiapicoplast and gametocytocidal screening to identify the mechanisms of action of compounds within the malaria box. Antimicrob Agents Chemother. 2014;58: 811–819.

29. Olivares AO, Baker TA, Sauer RT. Mechanistic insights into bacterial AAA+ proteases and protein-remodelling machines. Nat Rev Micro. 2016;14: 33–44.

30. Kim YI, Levchenko I, Fraczkowska K, Woodruff RV, Sauer RT, Baker TA. Molecular determinants of complex formation between Clp/Hsp100 ATPases and the ClpP peptidase. Nat Struct Biol. 2001;8: 230–233.

31. Bakkouri El M, Rathore S, Calmettes C, Wernimont AK, Liu K, Sinha D, et al. Structural insights into the inactive subunit of the apicoplast-localized caseinolytic protease complex of Plasmodium falciparum. J Biol Chem. 2013;288: 1022–1031.

32. AhYoung AP, Koehl A, Vizcarra CL, Cascio D, Egea PF. Structure of a putative ClpS N-end rule adaptor protein from the malaria pathogen Plasmodium falciparum. Protein Sci. 2016;25: 689–701.

33. Sass P, Josten M, Famulla K, Schiffer G, Sahl H-G, Hamoen L, et al. Antibiotic acyldepsipeptides activate ClpP peptidase to degrade the cell division protein FtsZ. Proc Natl Acad Sci. 2011;108: 17474–17479.

34. Drew ME, Banerjee R, Uffman EW, Gilbertson S, Rosenthal PJ, Goldberg DE. Plasmodium Food Vacuole Plasmepsins Are Activated by Falcipains. J Biol Chem. 2008;283: 12870–12876.

35. Russo I, Oksman A, Goldberg DE. Fatty acid acylation regulates trafficking of the unusual Plasmodium falciparum calpain to the nucleolus. Mol Microbiol. 2009;72: 229–245.

36. Liu J, Gluzman IY, Drew ME, Goldberg DE. The role of Plasmodium falciparum food vacuole plasmepsins. J Biol Chem. 2005;280: 1432–1437.

37. Klemba M, Gluzman I, Goldberg DE. A Plasmodium falciparum dipeptidyl

aminopeptidase I participates in vacuolar hemoglobin degradation. J Biol Chem. 2004;279: 43000–43007.

A

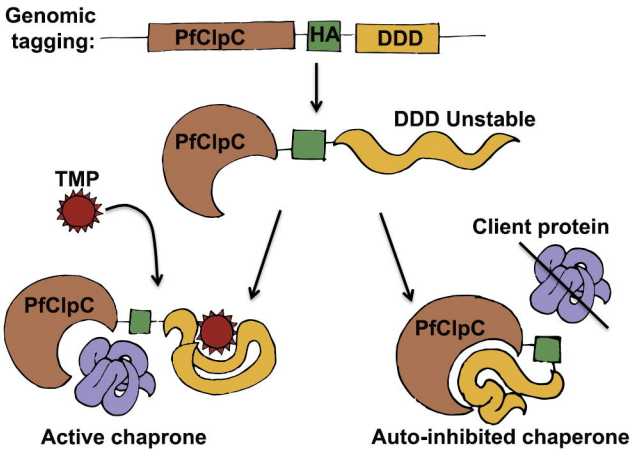
Genomic tagging:
PfClpC
HA
DDD
PfClpC
DDD Unstable
TMP
Client protein
PfClpC
PfClpC
Active chaprone
Auto-inhibited chaperone

C

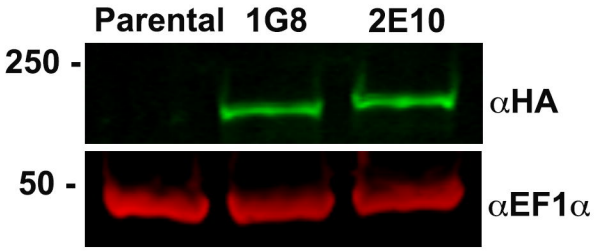
Parental
1G8
2E10
250 -
αHA
50 -
αEF1α

B

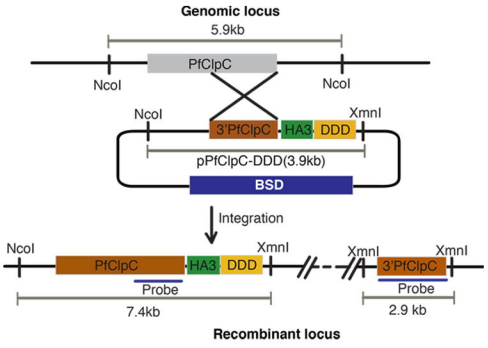
Genomic locus
5.9kb
PfClpC
NcoI
NcoI
NcoI
XmnI
3'PfClpC
HA3
DDD
pPfClpC-DDD(3.9kb)
BSD
Integration
NcoI
PfClpC
HA3
DDD
XmnI
XmnI
XmnI
3'PfClpC
Probe
Probe
7.4kb
2.9 kb
Recombinant locus

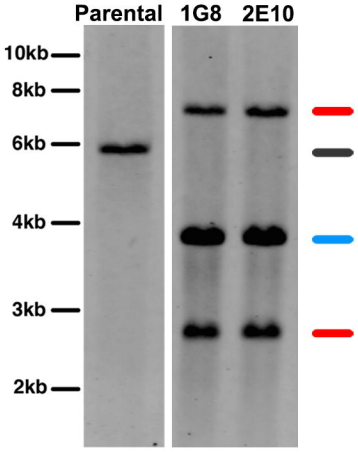
Parental
1G8
2E10
10kb
8kb
6kb
4kb
3kb
2kb

D

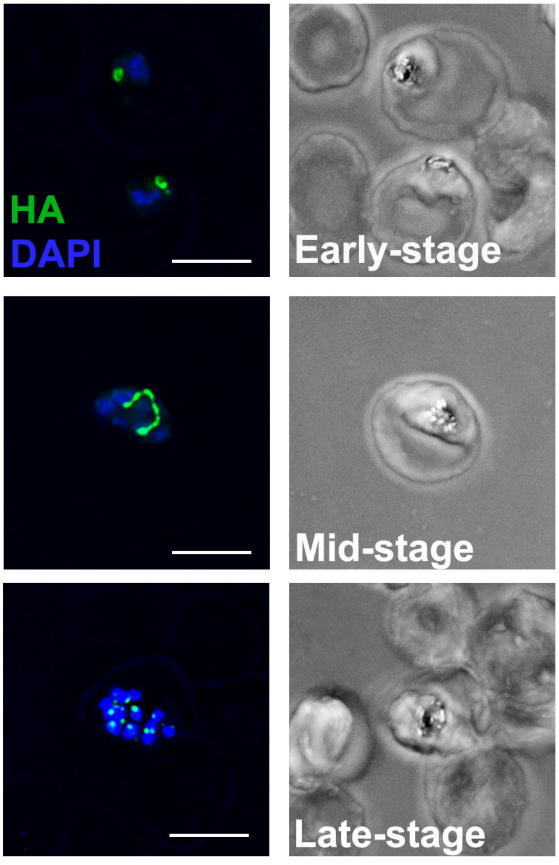
HA
DAPI
Early-stage
Mid-stage
Late-stage

A

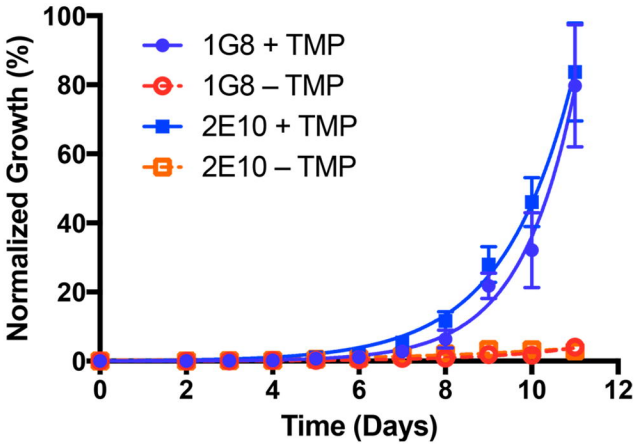
Normalized Growth (%)
100
80
60
40
20
0
1G8 + TMP
1G8 – TMP
2E10 + TMP
2E10 – TMP
0
2
4
6
8
10
12
Time (Days)

B

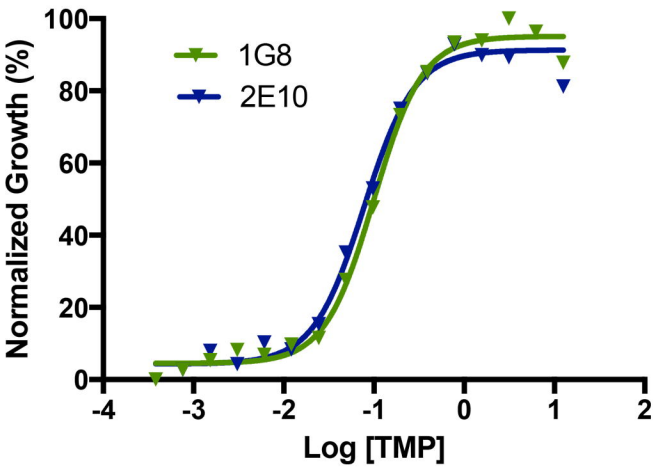
Normalized Growth (%)
100
80
60
40
20
0
1G8
2E10
-4
-3
-2
-1
0
1
2
Log [TMP]

C

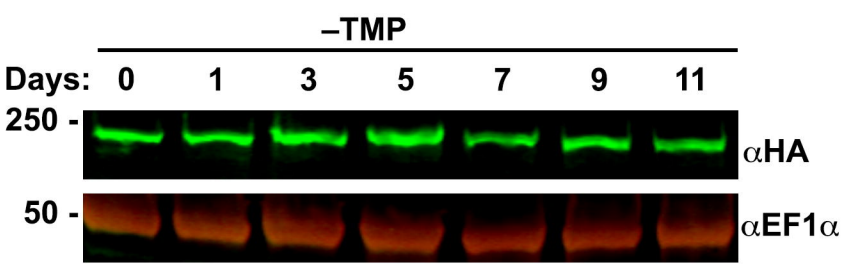
–TMP
Days: 0 1 3 5 7 9 11
250 -
αHA
50 -
αEF1α

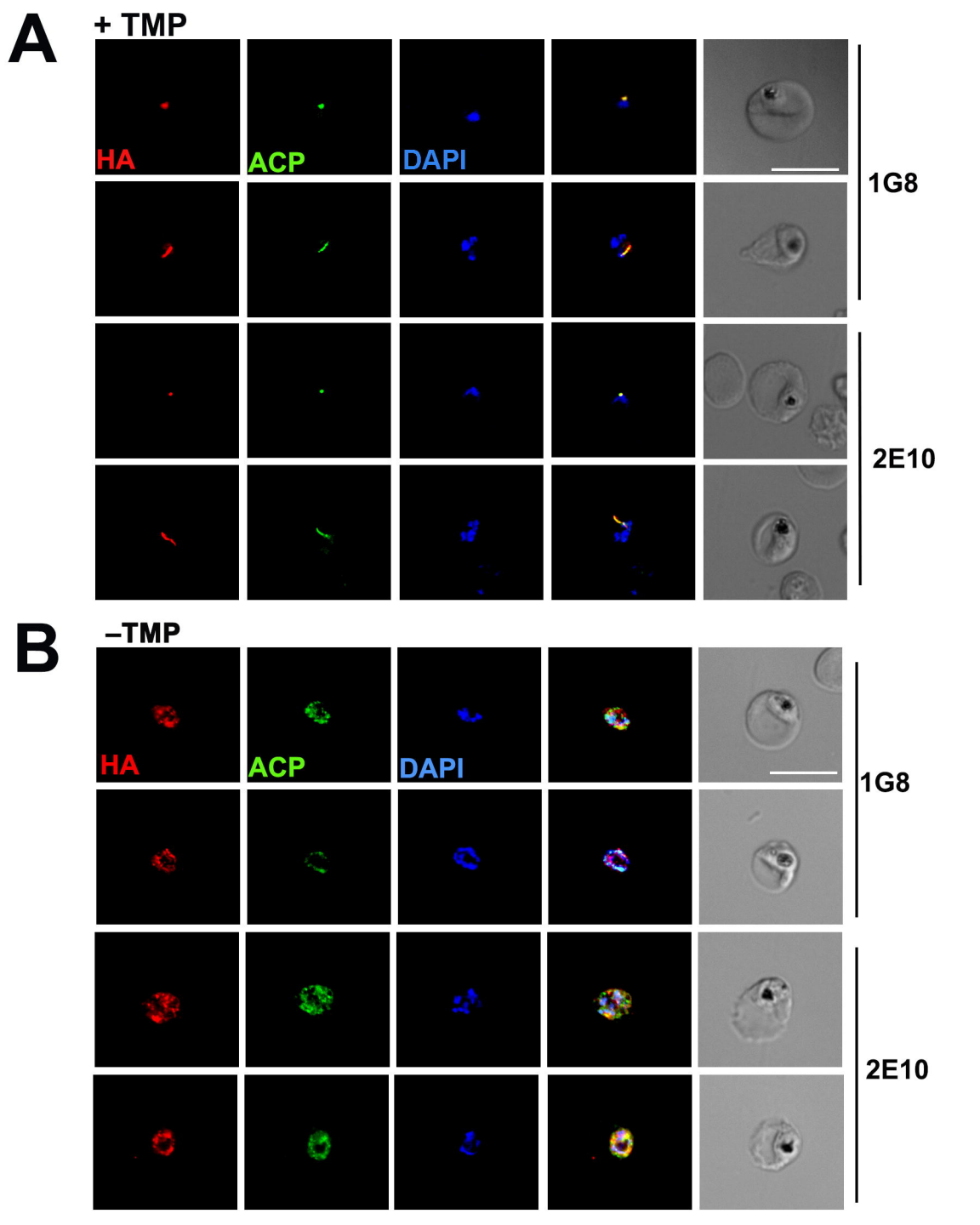
A
+ TMP
HA
ACP
DAPI
1G8
2E10
B
–TMP
HA
ACP
DAPI
1G8
2E10

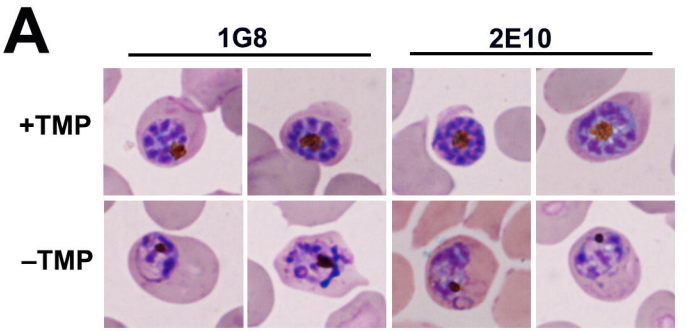
A
1G8
2E10
+TMP
–TMP

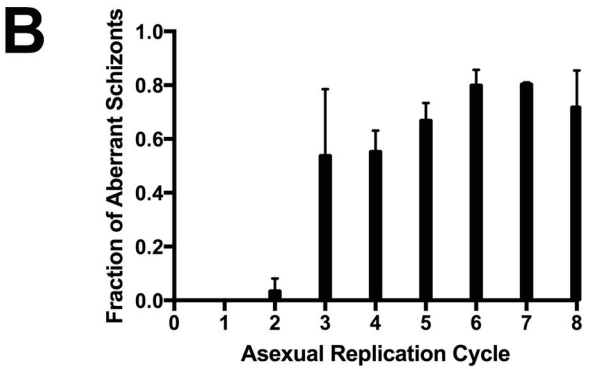
B
Fraction of Aberrant Schizonts
1.0
0.8
0.6
0.4
0.2
0.0
0
1
2
3
4
5
6
7
8
Asexual Replication Cycle

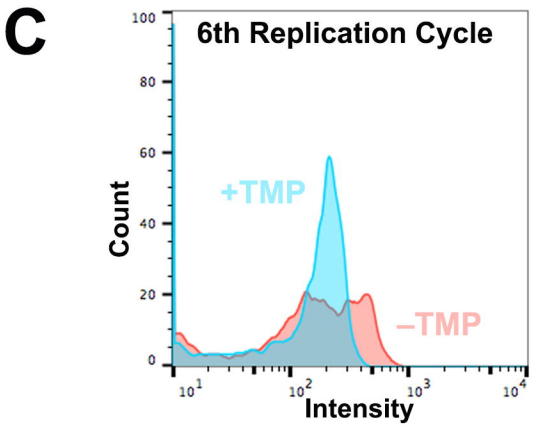
C
6th Replication Cycle
Count
100
80
60
40
20
0
+TMP
–TMP
10^1
10^2
10^3
10^4
Intensity

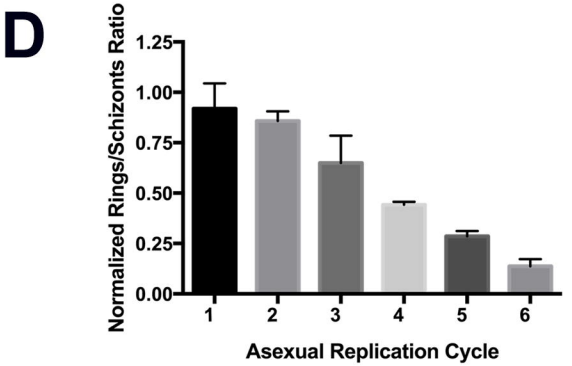
D
Normalized Rings/Schizonts Ratio
1.25
1.00
0.75
0.50
0.25
0.00
1
2
3
4
5
6
Asexual Replication Cycle

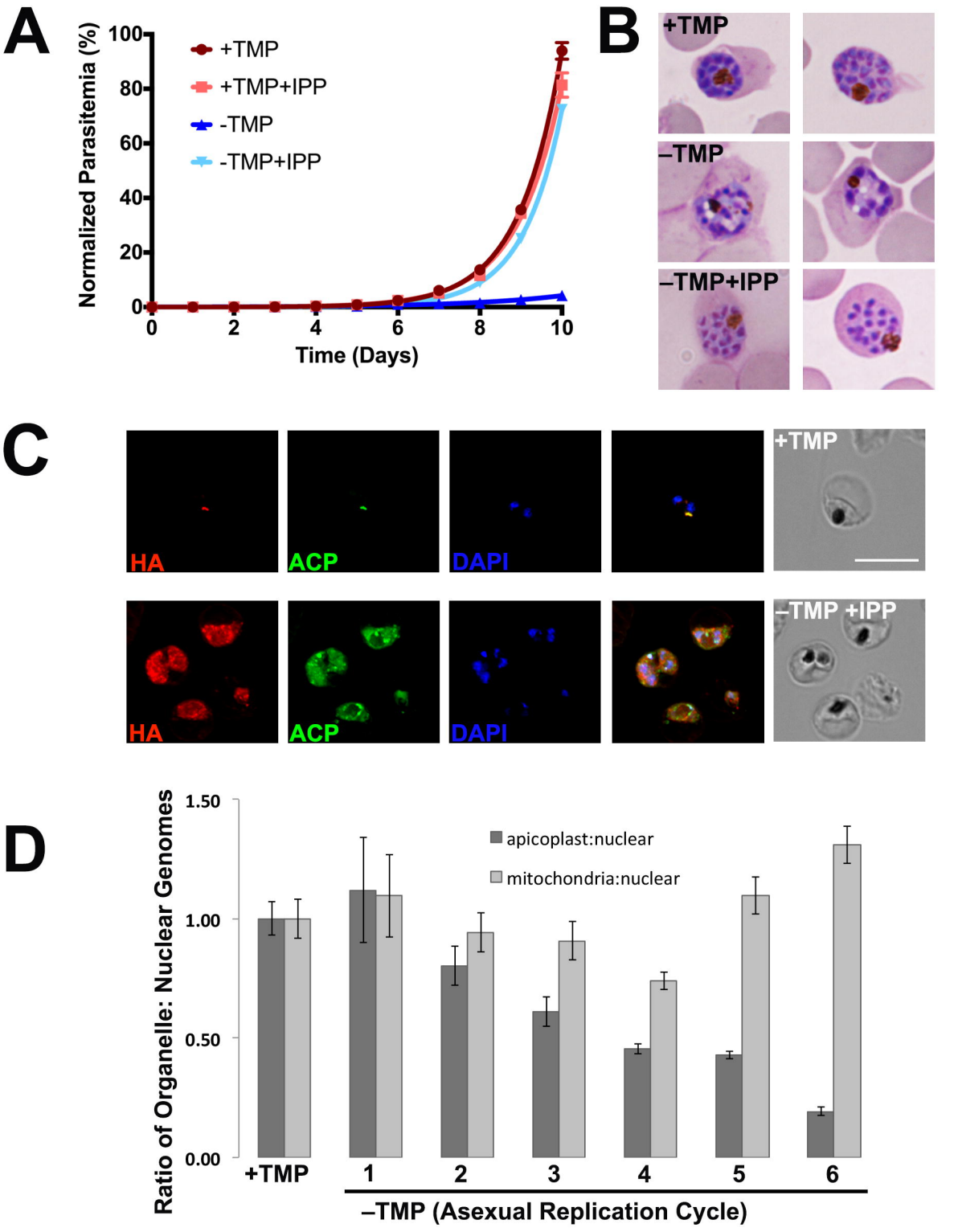
A
Normalized Parasitemia (%)
100
80
60
40
20
0
+TMP
+TMP+IPP
-TMP
-TMP+IPP
0
2
4
6
8
10
Time (Days)
B
+TMP
–TMP
–TMP+IPP
C
HA
ACP
DAPI
+TMP
HA
ACP
DAPI
–TMP +IPP
D
Ratio of Organelle: Nuclear Genomes
1.50
1.00
0.50
0.00
apicoplast:nuclear
mitochondria:nuclear
+TMP
1
2
3
4
5
6
–TMP (Asexual Replication Cycle)

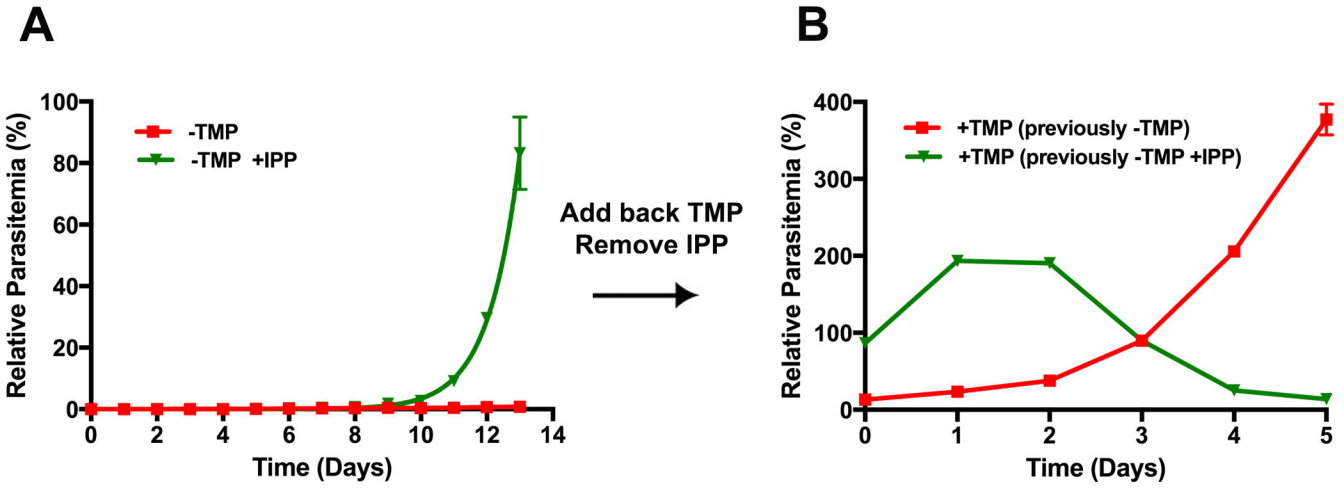
A
B
Relative Parasitemia (%)
100
80
60
40
20
0
-TMP
-TMP +IPP
0
2
4
6
8
10
12
14
Time (Days)
Add back TMP
Remove IPP
Relative Parasitemia (%)
400
300
200
100
0
+TMP (previously -TMP)
+TMP (previously -TMP +IPP)
0
1
2
3
4
5
Time (Days)